

Speed Control Algorithm of Pmsm for Compressor Load

Shwetha A¹, Dr. S G Srivani²

¹Student, Department of EEE, RV college of Engineering, Bengaluru, Karnataka.

²Associate Professor and Associate PG Dean, Department of EEE, RV College of Engineering, Bengaluru, Karnataka.

Submitted: 10-06-2021

Revised: 23-06-2021

Accepted: 26-06-2021

ABSTRACT: Permanent Magnet Synchronous Motor (PMSM) plays a significant role in Heating, Ventilation and Air Conditioning (HVAC) system. The compressor is an integral part of HVAC system and is driven by compressor load. The rotor position information is essential to achieve the speed regulation of PMSM based on the load requirements. The mechanical sensor such as encoder or resolver provides the necessary information of rotor position. However, the use of sensors increases the cost, size and hardware wiring complexity of overall drive system. Elimination of the sensors is highly motivated for sensorless control techniques to reduce the overall cost and size of a system. Hence, a speed control algorithm of PMSM by using Extended Kalman Filter (EKF) is proposed. The simulation is carried out for both sensed and EKF control technique in MATLAB/Simulink Software tool.

I. INTRODUCTION

Typically, Heating Ventilating and Air Conditioning (HVAC) system consumes around 30% of the total energy in domestic buildings and 48% of the total energy requirements in domestic buildings in USA [1]. Since the majority of power consumption in an HVAC system lies in compressor motor drive, the requirement of highly efficient motor is most significant. In recent years, the Permanent Magnet Synchronous Motor (PMSM) are progressively replacing the dc motors in performance applications such as robotics, Variable Speed Drives (VSD), aerospace actuators and industrial applications [2].

It offers the advantages of high accuracy, efficient, large torque inertia and power density ratio compared to induction motors for same output power capacity. The size of PMSM is compact and light weight that makes it preferable for certain high-performance applications [3].

To control the speed of PMSM based on the load requirement, it is essential to have the information of rotor position. It can be achieved either by sensed or sensorless control technique. In sensor-based control technique, usually a mechanical sensor like Hall effect sensor, Resolver or Encoder is used. However, using of these sensors increase the size, cost and hardware wire complexity [4][5].

Nowadays, the sensorless control techniques are in scope and comparable performance to sensed control. Basically, the sensorless control techniques can be categorized into methods based on the motor saliency and the fundamental model. The saliency-based control injects high frequency current or voltage signals into the motor and uses the corresponding signals to estimate the rotor position. This method is most suitable in the low-speed region and standstill condition of PMSM [8][9].

However, its performance has been degraded in medium or high-speed range of PMSM. The fundamental model based sensorless method estimates the back Electromotive Force (EMF) or flux linkage which contains the rotor position information, according to motor model by means of the Extended Kalman Filter (EKF), Rotor Flux Observer (RFO) and Sliding Mode Observer (SMO) [10] [11].

The mathematical model of Interior Permanent Magnet Synchronous Motor (IPMSM) is considered. An EKF sensorless control technique is employed to estimate the rotor position and speed. The tuning of covariance matrices involved in EKF is based on tuning guidelines [12] [13]. The Simulation is carried out for both sensed and EKF technique in MATLAB/ Simulink Software.

II. MATHEMATICAL MODEL OF PMSM

The Equation (2.1) represents the stator equations in d-q reference frame are:

$$V_{sq} = R_s i_q + L_q \frac{di_q}{dt} + \omega_e \lambda_{ds} \quad (2.1)$$

$$V_{sd} = R_s i_d + L_d \frac{di_d}{dt} - \omega_e \lambda_{qs} \quad (2.2)$$

The V_{sq} and V_{sd} are the d-axis and q-axis stator voltages. The i_d and i_q are d-axis and q-axis stator currents respectively. The R_s is the stator resistance and ω_e is the electrical rotor speed. The L_d and L_q are the d-axis and q-axis stator inductance respectively. The λ_{pm} is the flux linkage of permanent magnet rotor. The λ_{ds} and λ_{qs} are the d-axis and q-axis stator flux linkages. The flux linkages are expressed as

$$\lambda_{ds} = L_d i_d + \lambda_{pm} \quad (2.3)$$

$$\lambda_{qs} = L_q i_q \quad (2.4)$$

The electromagnetic torque is written as

$$T_e = \frac{3P}{2} (\lambda_{pm} i_q + (L_d - L_q) i_d i_q) \quad (2.5)$$

The mechanical speed is written as

$$\omega_m = \int \frac{1}{J} (T_e - T_L) dt \quad (2.6)$$

J is the inertia and P is the number of poles. The T_e is the electromagnetic torque and T_L is the load torque.

The electrical speed in terms of mechanical speed is written as

$$\omega_e = \frac{P}{2} \omega_m \quad (2.7)$$

The rotor position is written as

$$\theta_m = \int \omega_m dt \quad (2.8)$$

III. BLOCK DIAGRAM

The Block diagram of sensorless control technique is shown in Figure. 1.

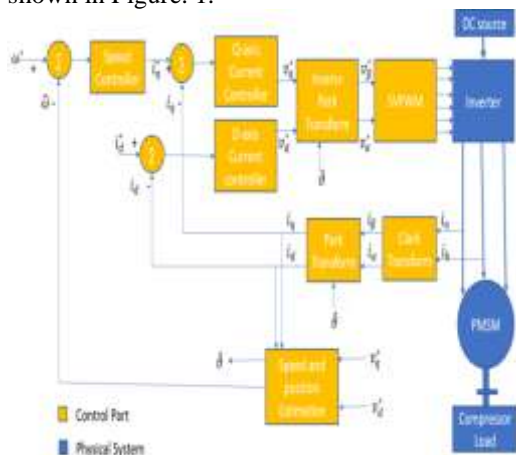


Figure. 1: Block Diagram of Sensorless Control of PMSM Drive

It consists of two parts:

1. Control system

2. Physical system

The control system consists of two inner current control loops and one outer speed control loop. The physical system consists of DC source, inverter, PMSM and compressor load. Based on the load requirement, the speed of PMSM is regulated by outer speed control loop. In sensorless control, there is an encoder which provides the information of rotor position and speed. This actual speed is compared with reference speed and error is fed to speed controller.

The speed controller generates the torque controlling current component. At the same time, any two motor phase currents are sensed by current sensors. The measured stator currents is transformed into α and β -axis current components using a Clarke transformation. The currents in α , β coordinates is transformed into the d, q reference frame using a Park transformation. The stator current torque and flux producing components are separately controlled in d, q rotating frame. The reference and actual d and q-axis current components are compared and error signals are fed to the respective current controllers.

The current controller generates the reference d and q-axis voltages and is transformed into reference α and β -axis voltages using inverse park transformation. From space vector modulation, three reference voltage signals are generated. The three reference voltage signals are compared with the carrier signals to generate the gate pulses and is fed to switches of inverter. In case of sensorless control, the encoder is eliminated. Instead, an EKF control algorithm is developed to estimate the rotor position and speed.

IV. METHODOLOGY

The block diagram of EKF control algorithm is shown in Figure. 2.

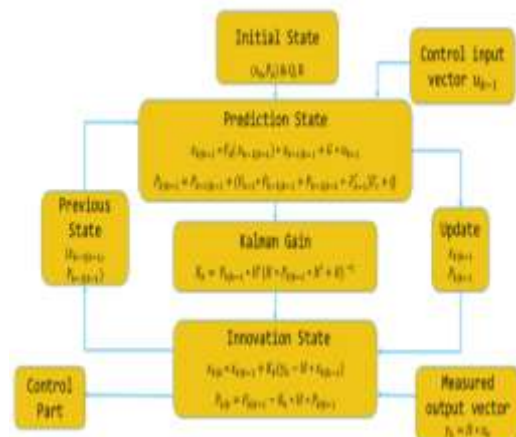


Figure. 2: Block diagram of EKF Control Algorithm

The steps involved in EKF control algorithm are as follows:

Step-1. Initialize the state vector x_0 and covariance matrices P_0 , Q and R .

P_0 - state covariance matrix

Q - System noise covariance matrix

R - Measurement noise covariance matrix.

Step-2. Predict the state vector $x_{k|k-1}$ and state covariance matrix $P_{k|k-1}$. In this step, the control input vector is updated by controller.

$$x_{k|k-1} = F_d(x_{k-1|k-1})x_{k-1|k-1} + Gu_{k-1} \quad (4.1)$$

$$P_{k|k-1} =$$

$$P_{k-1|k-1} + (F_{k-1}P_{k-1|k-1} + P_{k-1|k-1}F'_{k-1})T_c + Q \quad (4.2)$$

Step-3. Calculate the Kalman gain K_k by updating the estimated value of state covariance matrix $P_{k|k-1}$.

$$K_k = P_{k|k-1}H'(HP_{k|k-1}H' + R)^{-1} \quad (4.3)$$

Step-4. Innovate the state vector $x_{k|k}$ and state covariance matrix $P_{k|k}$ by updating the estimated values $x_{k|k-1}$, $P_{k|k-1}$ and K_k .

$$x_{k|k} = x_{k|k-1} + K_k(y_k - Hx_{k|k-1}) \quad (4.4)$$

$$P_{k|k} = P_{k|k-1} - K_kHP_{k|k-1} \quad (4.5)$$

Step-5. Update the innovated state vector $x_{k|k}$ and state covariance matrix $P_{k|k}$ to the controller.

Step-6. The innovated values are updated as previous values $x_{k-1|k-1}$ and $P_{k-1|k-1}$ for next iteration of EKF algorithm.

V. SIMULATION RESULTS

The specifications of simulation model of sensed and sensorless control of PMSM as tabulated in Table.1

Table. 1: Specifications of simulation model of sensed and sensorless control of PMSM.

Submodules	Parameters	Ratings
DC Source	Voltage	650V
Inverter	Voltage	480V
	Current	40A
	Power	22kW
	Switching Frequency	4kHz
IPMSM	Voltage	460V
	Current	35.5A
	Power	30HP
	Stator Resistance	0.09Ω
	d-axis inductance	3.93mH
	q-axis inductance	6.6mH
	No. of Poles	8
Flux Linkage	0.439Wb	

The simulation results of EKF and sensed control of PMSM are compared and analyzed in this section. The EKF control algorithm is verified for various operating speed regions. Firstly, the algorithm is verified for motor rated speed of 1800rpm and full load condition of 118Nm. The waveforms of actual and estimated speed are shown in Figure. 3.

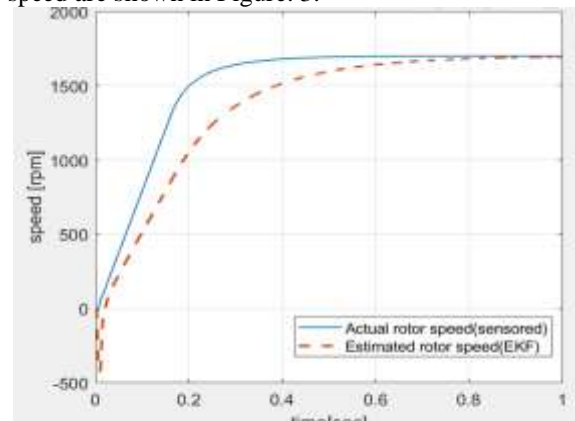


Figure. 3: Waveforms of Actual and Estimated speed for 1800rpm

It was observed from waveforms at $t=0.6$ sec, the actual speed reached the steady state and the speed value was found to be 1797rpm. The estimated speed value of 1779rpm was obtained. The EKF algorithm is verified for medium operating speed of 1000rpm and full load condition of 118Nm. The waveforms of actual and estimated speed are shown in Figure. 4.

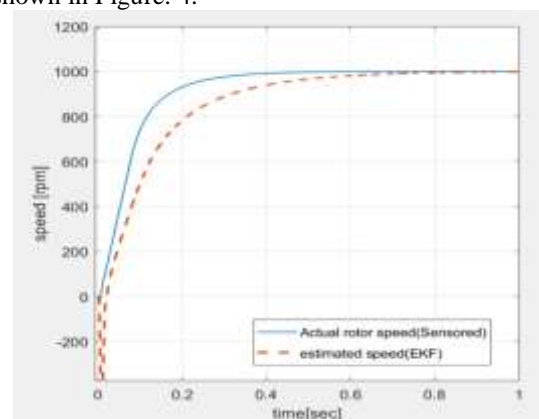


Figure. 4: Waveforms of Actual and Estimated speed for 1000pm

It was observed from simulation results; the speed is reached the steady state at $t=0.6$ sec. The value of actual speed of 998rpm and estimated speed of 994rpm were obtained. The EKF algorithm is verified for low operating speed of 300rpm and full load condition of 118Nm. The waveforms of actual and estimated speed are shown in Figure. 5.

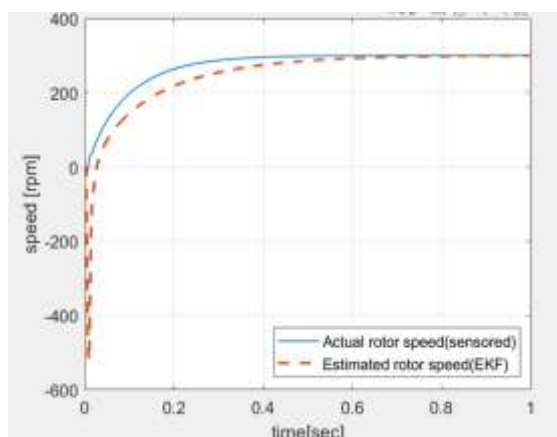


Figure 5: Waveforms of Actual and Estimated speed for 300rpm

It was observed from waveforms; the speed is reached the steady state at $t=0.6$ sec. The value of actual speed of 299rpm and estimated speed of 292rpm were obtained. At transient state, there is large error between the estimated and actual speed.

V. CONCLUSION

A speed control algorithm of PMSM using EKF technique is developed for rotor position and speed estimation in the proposed work. For full load condition of 118Nm, the error between the actual speed and estimated speed for steady state condition was less than 5%. For load condition of 59Nm, the error between the actual and estimated speed for steady state condition was less than 3%. The simulation results depict that the good accuracy of estimated speed for steady state conditions.

REFERENCES

- [1]. R. Lateb, J. Enon, and L. Durantay, "High speed, High Power Electrical Induction Motor Technologies for Integrated Compressors", International Conference on Electrical Machines and Systems, Tokyo, Japan, pp.1-5, November 2019.
- [2]. Hyunchai oh, Young Song, Kwan Yuhi Cho, Hag Wone and Byung Moon Han, "Initial rotor position detecting algorithm of PM synchronous motor using incremental encoder", IEEE ECCE Asia Downunder, Melbourne, VIC, Australia, pp. 681-686, August 2013.
- [3]. M Bourogaoui, Jlassi, S Khojet El Khil and H Bet AttiaSethom, "An effective encoder fault detection in PMSM drives at different speed ranges", International Symposium on Diagnostics for Electrical Machines, Power Electronics and Drives (SDEMPED), Guarda, Portugal, pp. 90-96, October 2015.
- [4]. Tomasz Rudnicki, Robert Czerwinski, Dariusz Polok and Andrzej Sikora, "Performance Analysis of PMSM Drive for Torque and speed Control", International Conference of Mixed Design of Integrated Circuits and Systems (MIXDES), Torun, Poland, pp. 562-566, August 2015.
- [5]. Sukanta Halder, Pramod Agarwal, and S P Srivasta, "MTPA based Sensorless Control of PMSM using position and speed estimation by Back-EMF method", International Conference on Power Systems (ICPS), New Delhi, India, pp. 1-4, October 2016.
- [6]. Qipeng Tang, Anwen Shen, Hanlin Shen, Wuhai Li and Xiangning He, "IPMSM Sensorless MTPA Control based on virtual q-axis Inductance by using Virtual High-frequency signal Injection", IEEE Transactions on Industrial Electronics, Vol. No. 67, Issue. No. 1, pp. 136-146, January 2019.
- [7]. Zhichen Lin, Xinmin Li, Zhiqiang Wang, Tingna Shi and Changliang Xia, "Minimization of Additional High-Frequency Torque Ripple for Square-Wave Voltage Injection IPMSM Sensorless Drives", IEEE Transactions on Power Electronics", Vol. No. 35, Issue No. 12, pp. 13345-13355, December 2020.
- [8]. Hang wu, Jianhuawu, Quigguo sun, Hongyuwang and Le zhang, "A Novel Sliding Mode Observer based Sensorless PMSM Control", International Conference on Electrical Machines and Systems (ICEMS), pp.1-5, August 2019.
- [9]. Quntao An, Jianqiu Zhang, Qi An, Xingya Liu, Alexander Shamekov, and Kaitao Bi, "Frequency-Adaptive Complex-Coefficient Filter-Based Enhanced Sliding Mode Observer for Sensorless Control of Permanent Magnet Synchronous Motor Drives", IEEE Transactions on Industrial Applications, Vol. No. 56, Issue No. 1, 335-343, January 2020.
- [10]. Mario Marchesoni, Massimiliano Passalacqua, Luis Vaccaro, Macro calvini and Macro Venturini, "An Improved Low-Noise Sensorless PMSM Drive able to Face Highly Intermittent Load Torque", International Symposium on Sensorless Control for Electrical Drives (SLED), pp.1-6, September 2019.
- [11]. Gao Tian, Yang Yan, Wang Jun, Zhou Yu Ru and Zhao Xiao Peng, "Rotor Position Estimation of Sensorless PMSM Based on

- Extended Kalman Filter”, International conference on Mechatronics, Robotics and Automation, Hefei, China, pp. 12-16, May 2018.
- [12]. Bologani, R. Oboe and M. Zigliotto, “Sensorless full-digital PMSM drive with EKF Estimation of Speed and rotor position”, IEEE Transactions on Industrial Electronics, Vol. No. 46, Issue No.1, pp. 184 -191, February 1999.
- [13]. S. Bolognani, L. Tubiana and M. Zigliotto, “Extended Kalman Filter Tuning in sensorless PMSM drives”, IEEE Transactions on Industrial Applications, Vol. No. 39, Issue. No. 6, pp. 1741-1747, November 2003.